Journal of Atomic and Molecular Sciences

Global Science Press

ISSN 2075-1303

Theoretical Study on Chemospecificity of $CF_3SO_3CF_2CF_3 + F^-$ Reactions

Received Oct. 22, 2017,
Accepted Dec. 12, 2017,

DOI: 10.4208/jams.102217.121217a

http://www.global-sci.org/jams/

Li Guo[a], Yulong Xu[a,*]

Abstract. DFT and ab initio methods are used to investigate why the reaction, $C(1)F_3S(2)O_2O(3)C(4)F_2C(5)F_3 + F^-$, results in the S-O cleavage chemospecifically. Three S_N2 channels, i.e. S-O cleavage and back- and front-side of C-O scission are predicted to occur. The F(11)and F(12) atoms of the $C(4)F_2$ group play the multiple roles in three paths. Multi-membered rings are formed in C-O rupture mechanisms due to the neighboring effect. The rate of S-O scission reaction is 10^{31} time as large as the rates of C-O rupture reactions. It is the combination of the irreversibility and the huge rate ratios to determine that S-O cleavage is chemospecific. This conclusion agrees well with the experimental results.

1. Introduction

Since the 1930s, halonium ions have been known to be a great source for unique synthetic pathways and insight into reaction mechanisms[1]. Organofluorine compounds have found widespread applications in diverse areas such as polymers, liquid crystals, and agricultural and medicinal chemistry[2-6]. Partial or full fluorination provides distinctive physicochemical properties to an organic molecule that can be attributed to the special properties of the carbonfluorine (C-F) bond[6]. Fluorine is the most electronegative (electron-attracting) element of the periodic table, so the C-F bond is highly polarized. Because of its small size and its high electronegativity, fluorine's electrons are poorly polarizable, and organofluorine compounds generally interact with other atoms or molecules only through rather weak electrostatic interactions[7,8]. The S_N2 nucleophilic substitution reaction is one of the most extensively studied chemical reactions in solution.

Hydrolysis of sulfonic ester RSO_2OR' is a S_N2 reaction[9], and the R'-O cleavage is much more likely than S-O cleavage when R' is alkyl. On the other hand, the S-O bond is much more likely to cleave when R' is aryl[9,10]. Such chemospecificity has also been found in the nucleophilic substitutions at perfluoro- and polyfluoro-sulfonic ester. In reaction (I), as shown by the experiments and theoretical study[11a, 11c], the nucleophile, such as F^-, attacks $RFSO_3CH_2R'F$ at the α-carbon atom, leading to the C-O cleavage exclusively. But reaction (Π) leads to the S-O cleavage solely[11b]. Such chemospecificity was ascribed to the screen effect and the electron repulsion between F^- and two fluorine atoms on the α-carbon atom. It is due to reaction (III) that reaction (II) can lead, specifically, to the S-O cleavage. Therefore, it is necessary to theoretically understand the chemospecificity of reactions (I) and (II) as well as to detail the roles of the α-group and β-group. In this paper, the DFT and ab initio methods (HF and MP2) are used to investigate reaction (II), and the theoretical research on the reaction (I) had been reported in this journal.

$$R_FSO_3CH_2R'_F + Nu^- \xrightarrow[\text{Cleavage}]{\text{C-O}} R_FSO_3^- + NuCH_2R'_F \quad (I)$$

$$R_FSO_3CF_2R'_F + Nu^- \xrightarrow[\text{Cleavage}]{\text{S-O}} R_FSO_2Nu + {}^-OCF_2R'_F \quad (II)$$

$$^-OCF_2R'_F \rightarrow R'_FCOF + F^- \quad (III)$$

There are three ways for F^- to attack $C(1)F_3S(2)O_2O(3)C(4)F_2C(5)F_3$ (PFS): (i) at the S atom from the backside of the O(3) atom, denoted as $S_N2(S)$; (ii) at the α-C atom from the backside of the O(3) atom(the S_N2 (C-B) mechanism); (iii) at the α-C atom from the frontside of the O(3) atom, denoted as S_N2(C-F). As the strongly electron-withdrawing group, two F atoms in the $C(4)F_2$ group play the multiple roles in three reaction paths. Their roles in determining chemospecificity of the reaction are particularly interesting. The multiple electrophilic centers are involved in the C-O scission reactions. At last, the kinetic analysis is performed.

2. Calculation Method

All computations are done using the Gaussian 09 program package[12]. The reactants, products, intermediates and transition states are optimized using B3LYP at 6-31+G* level. The harmonic vibration frequencies are calculated with the same method, and each transition state is characterized by one imaginary frequency. Afterwards, the IRC (intrinsic reaction coordinate) method[13] is used to track minimum energy path from transition state to the corresponding local minima.

In each of three S_N2 reactions, the charge, which is located to F^- before reaction, becomes dispersed over a somewhat larger area in the reactant complex and transition state (Figure 2.1). The solvent effects on the reaction are examined using the SCRF method [14], but those are so slight that discussion will not be presented in this work.

[a] School of Chemistry and Pharmaceutical Engineering, Qilu University of Technology(Shandong Academy of Sciences), Jinan，Shandong 250353, China
[b] School of science, Qilu University of Technology(Shandong Academy of Sciences), Jinan，Shandong 250353, China
*Corresponding author. Email:yulongxu@163.com

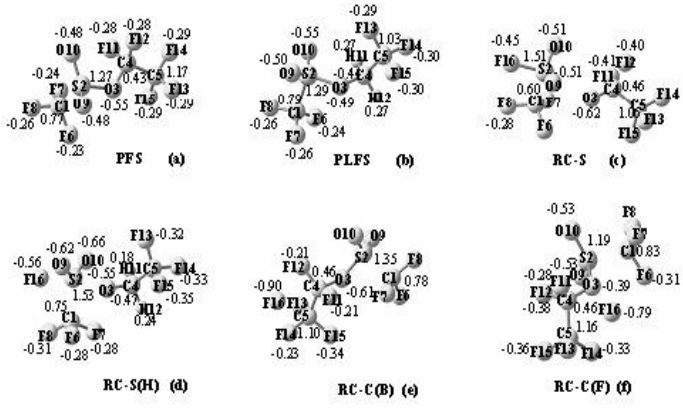

Figure 2.1: The Mulliken atomic charges obtained at B3LYP/6-31+G* level (PFS refers to a perfluoroethylsulfonate $CF_3SO_3CF_2CF_3$ and PLFS denotes a polyfluoroethylsulfonate $CF_3SO_3CH_2CF_3$.)

3. Results and discussion

3.1 The C-O Cleavage Mechanism.

As early indicated by March [9a], it is impossible for the frontside S_N2 mechanism to be observed. Recently, however, some experimental and theoretical chemists indicated that the frontside S_N2 mechanism is possible[9b,15]. In this work, it seems to be a possible way for F^- to attack PFS at the C(4) atom from the front side of the O(3) atom besides the well-know backside S_N2 mechanism.

3.1.1 The Backside S_N2 Mechanism.

In this mechanism, reactant complex, transition and product complex are denoted as RC-C(B), TS-C(B) and PC-C(B) respectively. RC-C(B) can be obtained from geometry optimization using B3LYP/6-31+G*, but it is almost impossible for the DFT method to locate a reasonable TS-C(B) although various efforts have been made. Fortunately, HF and MP2 methods are productive.

As shown in Figure 3.1.1, the conformations of RC-C(B), TS-C(B) and PC-C(B), obtained from the MP2 and HF/6-31+G*, are similar, but their geometrical data, such as the distances $r_{16,4}$ and $r_{16,5}$, the dihedral angle F(13)-C(5)-C(4)-F(16) as well as the bond angles ∠F(16)-C(5)-F(13) and ∠F(16)-C(4)-O(3), are obviously different from the corresponding those obtained from B3LYP/6-31+G*. For example, in RC-C(B), the distances $r_{16,5} \approx r_{16,4}$ (about 2.5 Å), and $r_{5,13} > r_{5,15} \approx r_{5,14}$ (HF and MP2). But the distances, $r_{16,4}$ (2.778 Å) < $r_{16,5}$ (3.130 Å) at B3LYP/631+G* level (the symbol "$r_{m,n}$" denotes the distance between the *m*th and *n*th atoms).

It will be found that the distance $r_{16,4}$ in the S_N2(C-B) mechanism is the longest of three possible mechanisms as far as the distance between F^- and the reaction center is concerned. As shown by the atomic charges (-0.28) of the F(11) and F(12) atoms (Figure 2.1a), the shielding effect, exerted by the F(11) and F(12) atoms, is a resistance to F^- attacking PFS at the atom C(4) from the backside of the O(3) atom, and DFT method is more sensitive to the shielding effect[16]. On the contrary, the group C(5)F3, as a neighbor of the reaction center C(4), may play a role in stabilizing RC-C(B) (neighboring effect) according to the dihedral angle F(13)-C(5)-C(4)-F(16) as well as to ∠F(16)-C(5)-F(13) and ∠F(16)-C(4)-O(3) in RC-B. In appearance, F^- attacks PFS at the C(4) and C(5) atoms, and a three-membered ring, F(16)-C(4)-C(5)-F(16), is formed in RC-C(B) and TS-C(B). In Figures 3.1.1a and 3.1.1b, for example, the dihedral angles F(13)-C(5)-C(4)-F(16) are 179.7° (HF/6-31+G*) and 179.8° (MP2/6-31+G*), ∠F(16)-C(4)-O(3) and ∠F(16)-C(5)-F(13) are: 177.7° and 179.2° (HF), 176.0° and 177.9° (MP2). Those mean that the F(16), C(4), C(5), O(3) and F(13) atoms in RC-C(B) are almost coplanar at HF and MP2/6-31+G* levels. In the meantime, the bond length $r_{5,13}$ is always longer than those $r_{5,14}$ and $r_{5,15}$. In the geometry obtained from DFT, the distance $r_{16,4}$ is the longest of three geometries of RC-B (Figures 3.1.1a~3.1.1c), and it is so long that the neighboring effect is weaker than that in each of two other geometries (Figures 3.1.1a and 3.1.1b). Correspondingly, $r_{16,4}$ = 2.778 Å < $r_{16,5}$ = 3.130 Å, ∠F(16)-C(5)-F(13) = 121.1° and the dihedral angle F(13)-C(5)-C(4)-F(16) = 116.5° (Figure 3.1.1c). The distance $r_{4,3}$ is getting longer while *r*16,4, is being shortened with the attack of F–, and a transition state is reached. In the meantime, the dihedral angle C(5)-C(4)-F(11)-F(12) is enlarged from about 130º to about 150° (Figures 3.1.1d and 3.1.1e), and $r_{16,4} < r_{16,5}$. In the vibrational model characterized by an imaginary frequency 560.7 cm^{-1}, as shown by the arrows in Figure 2f, the C(5)-C(4) bond looks like a pendulum, and the positions of the C(5), F(11) and F(12) atoms keep unchanged while the C(4)-F(16) and C(4)-O(3) bonds stretch. At last, the PC-C(B) is formed, and meanwhile the values of the dihedral angle C(5)-C(4)-F(11)-F(12) are -122.8° (MP2/6-31+G*), -122.6° (HF/6-31+G*) and –123.0° (B3LYP/6-31+G*). The configuration of molecule is inverted in PC-C(B) (Figures 3.1.1g~3.1.1i).

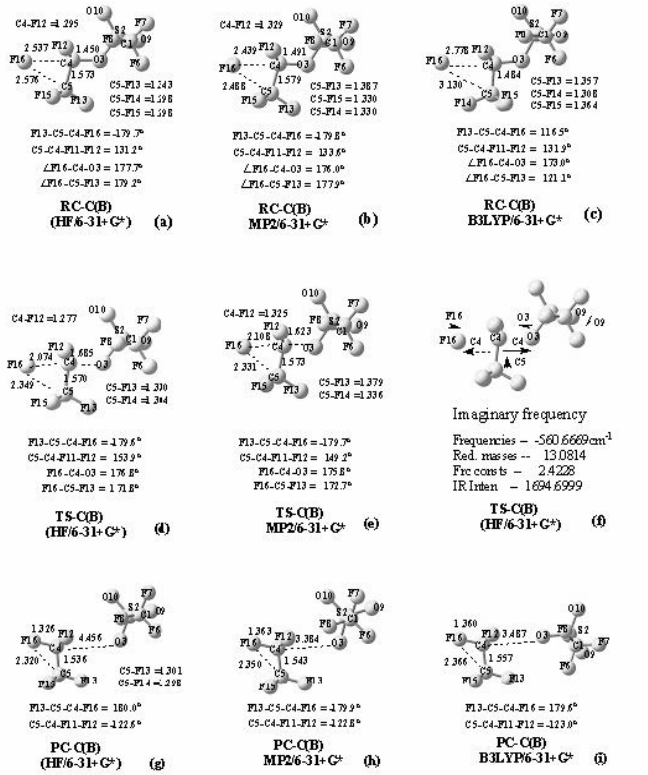

Figure 3.1.1: The Newman projections, looking down F12….F11, for RC-C(B) and TS-C(B) obtained from geometry optimization using HF, MP2 and B3LYP at 6-31+G* level (the bond length unit in Å).

3.1.2 The Frontside SN2 Mechanism.

In this case, reactant complex, transition and product complex are denoted as RC-C(F), TS-C(F) and PC-C(F). Interestingly, as shown by the data in Figure 3.1.2a, the neighboring effect and the remote interaction between F^- and the group $C(1)F_3$ at HF/6-31+G* level are greater than at B3LYP/6-31+G*. Correspondingly, the seven atoms, denoted as F(16), C(4), F(12), C(5), F(15), C(1) and F(8), are almost coplanar, and the distances $r_{16,4}$ (2.591 Å) ≈ $r_{16,5}$ (2.654 Å) ≈ $r_{16,1}$ (2.781 Å). The F− attacks atoms C(4), C(5) and C(1) simultaneously. On the contrary, as shown by Figure 3.1.2b and 3.1.2c, the distance $r_{16,1}$ is 4.103 Å (B3LYP/6-31+G*) and it is much longer than $r_{16,4}$ and $r_{16,5}$. However, the bond angle ∠F(16)-C(4)-F(12) in RC-C(F) is about 176° no matter which method is used to optimize RC-C(F). The shielding effect, exerted by F(11) and F(12), in RC-C(F) should be weaker than that in RC-C(B). Correspondingly, the distance $r_{16,4}$ is 2.428Å (B3LYP/6-31+G*), which is shorter than the $r_{16,4}$ (2.778 Å) in RC-C(B) (Figure 3.1.1c). Interestingly, so called frontside S_N2 reaction seems to be an exchange reaction of F^- (F(16)) and the F(12) atom on the basis of the following results (Figure 3.1.2): the dihedral angle C(5)-C(4)-O(3)-F(11) being enlarged from about -130° in RC-C(F) to about -170° in TS-C(F); the distance $r_{4,12}$ in TS-C(F) is greater than that in RC-C(F). However, the length of the bond C(4)-F(12) keeps unchanged during the period of the vibration characterized by its imaginary frequency. This vibrational model, together with the great difference in the distance $r_{4,3}$ between TS-C(F) and RC-C(F), confirms that TS-C(F) does be a transition state of the reaction leading to C-O cleavage. In fact, as shown by the conformations of TS-C(F) and PC-C(F) and by their geometrical data (Figures 3.1.2d and 3.1.2e), the products result from leaving of the group OSO2CF3 from the front side of the F(16) (F^-) atom.

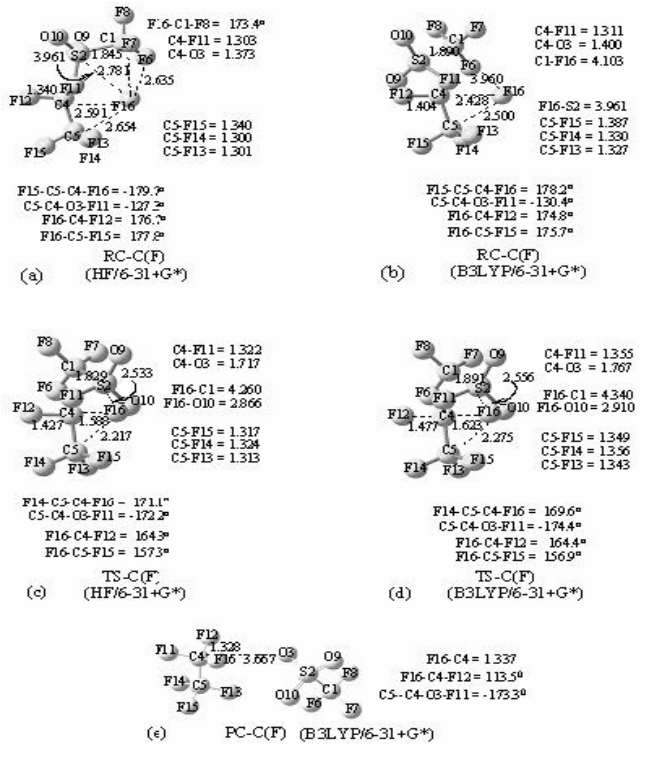

Figure 3.1.2: Optimized geometries of various species involved in the frontside S_N2 reaction leading to the rupture of the C-O bond (the bond length unit in Å).

Strikingly, the distances $r_{16,4}$ in TS-C(F) is much shorter than in RC-C(F), and it is so short that the neighboring effect seems to put out of action according to the following results: $r_{4,13} \approx r_{4,14} \approx r_{4,15}$ in TS-C(F) although $r_{16,5}$ in TS-C(F) < $r_{16,5}$ in RC-C(F), and $r_{16,5}$ in TS-C(F) (Figure 3.1.2) < $r_{16,5}$ in TC-C(B) (Figure 3.1.1). In the meantime, the distance $r_{16,2}$ (about 2.5 Å) in TS-C(F) is also shorter than those [3.205 Å (HF) and 3.961 Å (B3LYP/ 6-31+G*)] in RC-C(F), and a multi-membered ring, composed of the F(16), C(5), C(4), and S(2) atoms, is formed. Correspondingly, the conformation of TS-C(F), as well as most of its geometrical data, is no longer an artifact of a specific computation method. In appearance, the remote interaction between the F(16) and S(2) atoms plays an important role in determining the conformation of RC-C(F).

Particularly, the distance $r_{16,4}$ (about 1.6 Å) in TS-C(F) (about 1.6 Å) is much shorter than that (about 2.1 Å) in TS-C(B) (in Figure 3.1.1), and the difference in the value of $r_{16,4}$ between RC-C(F) and TS-C(F) is two times as large as that between RC-C(B) and TS-C(B).

3.2 The S-O Cleavage Mechanism.

In the $S_N2(S)$ mechanism, the reactant complex, transition state and product complex are, respectively, denoted as RC-S, TS-S and PC-S.

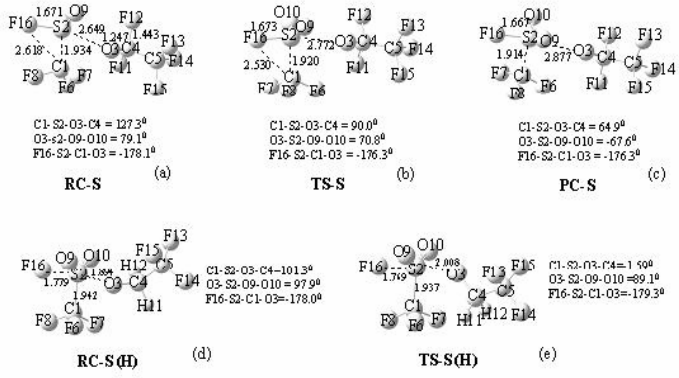

Figure 3.2.1: The geometries for various species involved in the S-O rupture reaction are obtained from B3LYP/6-31+G* (RC-S(H) and TS-S(H) means that the F11 and F12 atoms in RC-S have been replaced with two H atoms)

According to the atomic charges of the atoms in PFS (Figure 2.1a), the positive charge (1.17) of the atom C(5) is greater than that (0.43) of the C(4) atom, and all F atoms have negative charge (about –0.23 ~ -0.29). Therefore, the electrophilicity of C(5) is stronger than that of C(4). It may be a reason why a multi-membered ring is formed in RC-C(B) and RC-C(F). Furthermore, the positive charge (1.27) of the S(2) atom in PFS is greater than that of C(5). And the eletrophilicity of the S(2) atom should be much greater than those of all carbon atoms in PFS. Correspondingly, the distance $r_{16,2}$ is the shortest of three mechanisms as far as the distance between F− and reaction center is concerned. In addition, the negative charge of each of two oxygen atoms O(9) and O(10) is –0.48, it is so great that the repulsion between F^- and two oxygen atoms O(9) and O(10) is greater than that between F^- and two fluorine atoms F(11) and F(12). As a result, the values of the dihedral angle O(3)-S(2)-O(9)-O(10) for RC-S, TS-S and PC-S (Figures 3.2.1a ~ 3.2.1c) are all less than 90o (that for PFS is about 128.9°). The configuration of molecule is inverted (Walden inversion) as early as RC-S. Interestingly, the bond lengths $r_{4,11}$ and $r_{4,12}$, are lengthened from 1.350 Å in PFS to about 1.443 Å in RC-S, and the

bond length $r_{3,4}$, is shortened from 1.384 Å to 1.247 Å (Figure 3.2.1a) The lengths of these disturbed bonds almost keep unchanged until the formation of the products. In the meantime, 0.55electron charge of F(16) is dispersed to the O(3), C(4), F(11) and F(12) atoms, and the absolute values of the atomic charges of the atoms F(11) and F(12) increase from –0.28 in PFS to –0.40 in RC-S (Figures 2.1a and 2.1c). To understand the role of the F(11) and F(12) atoms in the S_N2(S) mechanism, the reactant complex, denoted as RC-S(H), and transition state, TS-S(H), of reaction $CF_3SO_3C\mathbf{H}_2CF_3 + F^-$ are optimized at B3LYP/6-31+G* (the symbols RC-S(H) and TS-S(H) mean that the F(11) and F(12) atoms in each of RC-S and TS-S have been replaced with two hydrogen atoms). As indicated by the geometrical data presented in Figures 3.2.1d and 3.2.1e, the bond lengths $r_{4,11}$ and $r_{4,12}$ in each of RC-S(H) and TS-S(H) almost keep unchanged during the period of F^- (F(16)) attacking PLFS at the S(2) atom. Correspondingly, the values of dihedral angle O(3)-S(2)-O(9)-O(10) for RC-S(H) and TS-S(H) are 97.9° (> 90° in Figure 3.2.1d) and 89.1° (< 90° in Figure 3.2.1e), and meanwhile 0.44 atomic charge of the F^- is dispersed to three oxygen atoms O(3), O(9) and O(10) (Figures 2.1b and 2.1d). Two fluorine atoms F(11) and F(12) in PFS, as the strongly electron-withdrawing groups and as the groups with the leaving ability, are pulling the O(3) atom away from the S(2) atom while F^- is attacking PFS at the S(2) atom. As a result, $-OC\mathbf{F}_2CF_3$ is a better leaving group than $-OC\mathbf{H}_2CF_3$.

3.3. Potential Energy Profile for the Reaction

The single point energy computation is performed, at MP2/6-311+G* level, for each ofvarious species obtained from the geometry optimization at B3LYP/6-31+G* level due to the following two reasons: (i) DFT methods have been found to systematically underestimate energy barrier[16]; (ii) it is practically difficult to optimize all species using the same method. On the basis of the data presented in Figure 3.3.1 and Table 3-1, the values of the activation energies for three attacking ways are: (i) $\Delta E^{TS\text{-}S}$ RC-S = 1.637 kcal/mol (B3LYP/6-31+G*), 1.768 kcal/mol (MP2/6-311+G*), (ii) $\Delta E^{TS\text{-}C(B)}$ RC-C(B) = 1.004 kcal/mol (MP2/6-31+G*), 1.500 kcal/mol (MP2/6-311+G*); (iii) ΔETS-C(F)RC-C(F) = 11.692 kcal/mol (B3LYP/6-31+G*), 12.188 kcal/mol (MP2/6-311+G*) (The superscript "TS-S" and subscript "RC-S' in symbol $\Delta E^{TS\text{-}S}$ RC-S, for example, mean that the activation energy *E** is the energy difference ($E^{TS\text{-}S} - E^{RC\text{-}S}$) between TS-S and RC-S). Strikingly, $\Delta E^{TS\text{-}S}$ RC-S (1.768 kcal/mol) ≈ $\Delta E^{TS\text{-}S}$ PC-S (1.805 kcal/mol), but $\Delta E^{TS\text{-}C(F)}$ RC-C(F) (12.188kcal/mol) << $\Delta E^{TS\text{-}C(F)}$ PC-C(F) (76.771 kcal/mol), $\Delta E^{TS\text{-}C(B)}$ RC-C(B) (1.5 kcal/mol) << $\Delta E^{TS\text{-}C(B)}$ PC-C(B) (339.0 kcal/mol). The S_N2 reaction leading to the S-O cleavage is reversible, and the eventual products should be resulted from the C-O cleavage. In fact, as shown by the experiments [3], the reaction, resulting in the S-O cleavage, is followed by reaction (III). It is just due to reaction (III) that whole reaction via breaking of the S-O bond is irreversible. The activation energy for each of three attacking ways, as well as the differences in the value of the activation energy between three attacking ways, is small. Therefore, it is unreasonable to ascribe the chemospecificity of the reaction $CF_3SO_3CF_2CF_3 + F^-$ to the activation energy difference.

In the theoretical calculation, the S_N2 reaction is dealt as a two-step reaction. At the first step, reaction complex results from the interaction between PFS and F^-. In this case, the rate-determining step of whole S_N2 reaction only involves reactant complex (RC), and its reaction rate can be written as equation (1):

$$\nu = -d[RC]/dt = k[RC], \quad (1)$$

where [*RC*] is the concentration of RC, and *k* is rate constant. As far as the S_N2(C-F) and S_N2(S) reactions (Scheme 1) are concerned, we have equations (2) and (3).

$$v_s/v_{cf} = (k_s/k_{cf})([RC-S]/[RC-C(F)]), \quad (2)$$

$$k_s/k_{cf} = (A_s/A_{cf})e^{-(E^*_s - E^*_{cf})/RT}, \quad (3)$$

where v_{cf} and v_s are the rates of reactions S_N2(C-F) and S_N2(S), *kcf* and *ks* are their rate constants, E^*_s and E^*_{cf} are the activation energies, and $A_s/A_{cf} = 1$.

Table 3-1. Total energy *E*(including zero-point energy) and Enthalpy *H* are obtained from the geometry optimization at B3LYP/6-31+G*, and relative energy, denoted as Δ*E* and Δ*H*

Species		B3LYP/6-31+G*				MP2/6-311+G*	
		Total energies (hartree)	Δ*E* (kcal/mol)	Enthalpies (hartree)	Δ*H* (kcal/mol)	Total energies (hartree)	Δ*E* (kcal/mol)
R + F^-		-1636.7883957	0	-1636.661452	0	-1633.9276357	0
RC-S		-1636.8921351	-65.1	-1636.765978	-65.6	-1634.0253116	-61.3
TS-S		-1636.8893243	-63.3	-1636.764452	-64.6	-1634.022495	-59.5
PC-S		-1636.8921483	-65.1	-1636.766006	-65.6	-1634.0253709	-61.3
[a]P1-S + P2-S		-1636.8796232	-57.3	-1636.756408	-59.6	-1634.0065589.	-49.5
RC-C(F)		-1636.8127309	-15.3	-1636.686371	-15.6	-1633.9469316	-12.1
TS-C(F)		-1636.7940977	-3.6	-1636.671207	-6.1	-1633.927508	0.1
PC-C(F)		1636.9134286	-78.5	-1636.784699	-77.3	-1634.0472726	-75.1
[b]P1-C + P2-C		-1636.9096438	-76.1	-1636.783114	-76.3	-1634.0391295	-70.0
RC-C(B)		-1636.8032148	-9.3	-1636.675927	-9.1	-1633.942192	-9.1
[c]MP2/	RC-C(B)	-1633.269819				-1633.9470175	-12.2
6-31+G*	TS-C(B)	-1633.2682029				-1633.9446261	-10.7
	PC-C(B)	-1633.3703901				-1633.3703901	-349.7

[a] P1-S and P2-S are the products in reaction (II); [b] P1-C and P2-C are the products resulted from the C4-O3 cleavage; [c] RC-C(B), TC-C(B) and PC-C(B) are obtained from the geometry optimization at MP2/6-31+G* due to the DFT method being not productive for optimizing TS-C(B).

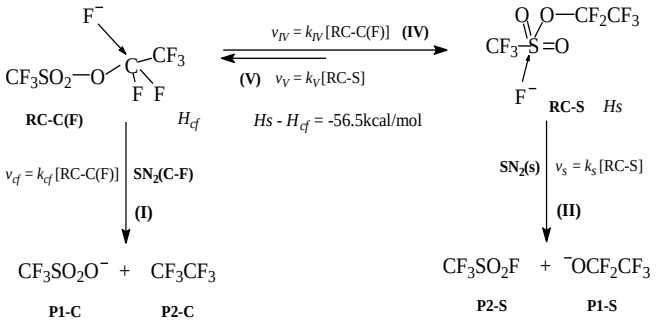

Scheme 1

It should be reasonable to suppose that there is a equilibrium between RC-S, RC-C(F) and RC-C(B) because these species result from the collision between F^- and PFS. According to the general relation between the activation energies and enthalpy change in the reaction[18], the constant *K* of the equilibrium between RC-S and RC-C(F), for example, can be expressed as equation (4):

$$K = [RC-S]/[RC-C] = k_{iv}/k_v = [(k_{iv})_\infty/(k_v)_\infty \, exp[-(H_s - H_{cf})/RT], \quad (4)$$

Where, k_{iv} and k_v are the rate constants of the reactions (IV) and (V) in Scheme 2, $(k_{iv})_\infty$ and $(k_v)_\infty$ are the rate constants when $T \to \infty$, and H_s and H_{cf} are the enthalpies for *RC–S* and *RC–C*(*F*). $[(k_{iv})_\infty/(k_v)_\infty] = 1$ because each of reactions (IV) and (V) is unimolecular. The ratio [*RC–S*]/[*RC–C*] in equation (2) is replaced with equation (4), we have equation (5):

$$v_s/v_{cf} \approx \left\{exp\left[-\left(\left(E_s^* - E_{cf}^*\right) - \left(H_s - H_{cf}\right)\right)/RT\right]\right\}, \qquad (5)$$

When *T* is about 400K[3], exp[-(H_s–H_{cf})/RT] = 0.745 × 10^{31}, and exp[-(E^*_s – E^*_{cf})/RT] = 1.879. Thus, the ratio v_s/v_{cf}, as well as the ratio v_s/v_{cb} of the S_N2(S) reaction rate to the S_N2(C-B) reaction rate, is about equal to exp[-(H_s –H_{cf})/RT] (0.745 × 10^{31}), and it is so huge that it is impossible for the products $CF_3SO_2O^-$ and CF_3CF_3, arising from the C-O cleavage, to be observed.

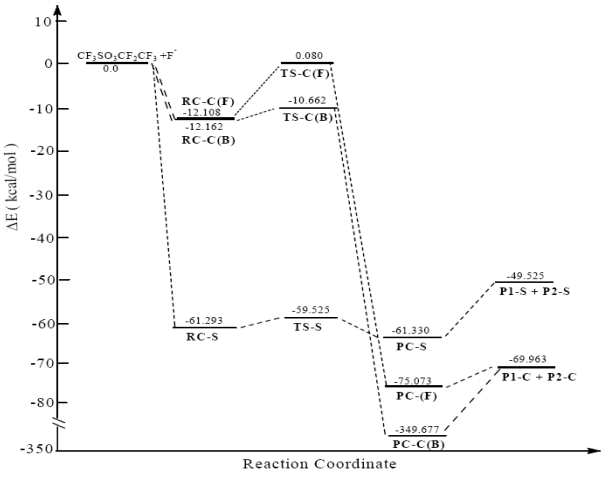

Figure 3.3.1: Energetic profile for the potential surface of the CF3SO3CF2CF3 + F− reaction at MP2/6-311+G*

4. Conclusions

The F(11) and F(12) play the multiple roles in three mechanisms, and their roles in determining chemospecificity of the reaction are particularly interesting. So called frontside S_N2 mechanism is initiated via a strong tendency of the F(12) atom to leave from the backside of the nucleophile F^-, but the eventual cleavage occurs in the C-O bond rather than in C(4)-F(12) bond because $-OSO_2CF_3$ is a better leaving group than the F(12) atom. The rate *vs* of the S_N2(S) reaction is 1031 times as large as each of rates v_{cf} and v_{cb} of the S_N2(C-B) and S_N2(C-F) reactions, which should be ascribed to the great differences in the enthalpy between RC-S, RC-C(F) and RC-C(B) rather than to the difference in the activation energy between three attacking ways. However, these huge ratios do not sufficiently ensure that the reaction leading to the S-O cleavage is chemospecific because the reaction, itself, is reversible.

Each of all F atoms in PFS has negative charge (about –0.25), and the shielding effect, exerted by the F(11) and F(12) atoms, is a resistance to F− attacking PFS at the C(4) atom from the back- or front-side of the O(3) atom. On the other hand, the F(11) and F(12) atoms are pulling the O(3) atom away from the S(2) atom while F^- is attacking PFS at the S(2) atom. Eventually, one of these two F atoms, a leaving group, is substituted as soon as the product, $-OCF_2CF_3$, results from breaking of the S-O bond, which makes whole reaction via the S-O cleavage irreversible. It is the combination of the irreversibility and the huge rate ratios to determine that the reaction leading to the S-O cleavage is chemospecific.

A multimember ring is formed when F attacks PFS at the C(4) atom from the back- and front-side of the O(3) atom via the neighboring effect and interaction between F^- and the remote groups C(1)F_3 and S(2)O_2. It is difficult to understand whether the neighboring effect and remote interactions promote the reaction or not, but it is reasonable, at least, to say that those may stabilize reactant complex and transition state.

Acknowledgements

This work was supported by the Natural Science Foundation of Shan dong Province (Grant No. ZR2016AM25)

References

[1] I. Roberts, G. E. Kimball, J. Am. Chem. Soc. 59 (1937) 947.
[2] P. Kirsch, Modern Fluoroorganic Chemistry: Synthesis, Reactivity, *Applications* Wiley-VCH, Weinheim, Germany, (2004).
[3] K. Uneyama, Organofl uorine Chemistry, Blackwell, Oxford, UK, 2006.
[4] U. Hennecke, Science 340 (2013) 41.
[5] M. D. Struble, M. T. Scerba, M. Siegler, T. Lectka, Science 340 (2013) 57.
[6] Liu F Y, Long Z W, Tan X F, et al. J. Mol. Model., 20 (2014) 2435.
[7] D. O'Hagan, Chem. Soc. Rev. 37, (2008) 308.
[8] R. Berger, G. Resnati, P. Metrangolo, E. Weber, J. Hulliger. Chem. Soc. Rev. 40, (2011) 3496.
[9] (a) J. March, Advanced Organic Chemistry, John Wily & Sons, Inc:New Work, 1992, p.497.
(b) K. P. C.Vollhardt, N. E. Schore, Organic Chemistry, W. H. Freeman and Company: New York, 1999.
(c) D. C. Nechers, M. P. Doyle, Organic Chemistry, John Wiley & Sons: New York, 1977.
(d) E. S. Gold, Mechanism and Structure in Organic Chemistry, Henry Holt and Company, Inc: New York, 1959.
[10] (a) S. Oae, T. Fukumoto, R. Kiritani, Bull. Chem. Soc. JPN. 36 (1963) 346.(b) W. Tagaki, T. Kurusu, S. Oae, Bull. Chem. Soc. JPN. 42 (1969) 2894.
[11] (a) Q.-Y. Chen, R.-X. Zhu, Z.-Z. Li, S.-D. Wang, W.-H. Huang, Acta. Chimica. Sinica, 40 (1982) 337.
(b) Q.-Y. Chen, S.-Z. Zhu, Acta. Chimica Sinica, 41 (1983) 1044.
(c) Guo, L., Yu, Z.-H., Chen, Q.-Y.; Zhu, R.-X.; J. Mol. Struc. (Theochem), 730 (2005) 143.
[12] M. J. Frisch, G. W. Trucks, H. B. Schlegel, et al. Gaussian 09, Revision A.02. Gaussian, Inc.: Wallingford CT, 2009.
[13] C. Gonzalez, H. B. Schlegel, J. Phys. Chem., 94 (1990) 5523.
[14] M. W. Wong, M. J. Frisch, K. B. Wiberg, Solvent effects. J. Am. Chem. Soc., 113 (1991) 4776
[15] (a) E. Uggerud, J. Org. Chem., 66 (2001) 7084.
(b) E. Uggerud, *Int.* J. Mass Spectrom, 182/183 (1999) 13.
(c) S. K. Goh, D. S. Marynick, Organometallics, 21 (2002) 2262.
(d) M. F. Bichelhaup, T. Ziegler, P. R. Schleyer, Organometallics, 14 (1995) 2288.
(e) P. R. Brooks, S. A. Harris, J. Chem. Phys., 117 (2002) 4220.
(f) M. N. Glukhovtsev, A. Pross, H. B. Schlegel, R. D. Bach, L. Radom, J. Am. Chem. Soc., 118 (1996) 11258.
[16] C. H. Choi, M. Kertesz, J. Phys. Chem. A, 101 (1997) 3823.
[17] (a) B. J. Lynch, P. L. Fast, M. Harris, D. G. Truhlar, J. Phys. Chem. A, 104 (2000) 4811.
(b) B. J. Lynch, D. G. Truhlar, J. Phys. Chem. A, 105 (2001) 2936.

(c) B. S. Jursic, J. Mol.Struc. (Theochem), 427 (1998) 137.
[18] (a) G.. W. Castellan, Physical Chemistry, Addison-Wesley Publishing Company, Inc: Japan, 1964.
(b) N. Isaacs, Physical Organic Chemistry, *A*ddison Wesley Longman Limited: London, 1996.